ORIGINAL RESEARCH PAPER

Application of Combined Cake Filtration-Complete Blocking Model to Ultrafiltration of Skim Milk

Mansour Kazemimoghadam [1,*], Zahra Amiri-Rigi [2]

[1]*Faculty of Chemistry and Chemical Engineering, Malek Ashtar University of Technology, Tehran, Iran*
[2]*Department of Chemical Engineering, South Tehran Branch, Islamic Azad University, Tehran, Iran*

ABSTRACT
Membrane ultrafiltration (UF) is widely used in dairy industries like milk concentration and dehydration processes. The limiting factor of UF systems is fouling which is defined as the precipitation of solutes in the form of a cake layer on the surface of the membrane. In this study, the combined cake filtration-complete blocking model was compared to cake filtration mechanism for flux data through ultrafiltration of skim milk at constant flow rate. The resistance data also was modeled using cake filtration model and standard blocking model. The effect of different trans-membrane pressures and temperatures on flux decline was then investigated. Based on the results obtained here, the combined complete blocking-cake formation model was in excellent agreement with experimental data. The cake filtration model also provided good data fits and can be applied to solutions whose solutes tend to accumulate on the surface of the membrane in the form of a cake layer. With increasing pressure, the differences between the model and experimental data increased.

Keywords: *Flux Decline; Fouling; Milk Concentration; Modeling; Ultrafiltration*

INTRODUCTION

Skim milk concentration is an important filtration process in the food industry in which milk proteins are separated from other components of skim milk, such as salt, lactose, microsorganisms, and water. This process is widely used in cheese making [1, 2] and production of milk protein concentrates, such as whey, which is a vital ingredient used in infants' food and also valuable for preparing barley sourdough [3, 4, 5].

Many techniques can be used for skim milk concentration, such as spray drying, freeze drying, evaporation, salt, pH and heat treatment. However, for large-scale milk concentration, these methods are neither economical nor suitable because they degrade the nutritional properties of the final product and their overall productivity is also very low. Deterioration of the natural state of the milk

due to these traditional techniques is associated with the exposure to heat treatment and changing the salt and pH content of the feed [6, 7].

Instead, ultrafiltration membrane contactors are widely applied in milk concentration and dehydration processes. These filtration systems have attracted great attention over the past few decades not only for their improved capacity and efficiency but also for their considerable decrease in power consumption [8-12]. In fact, ultrafiltration processes have several advantages over traditional concentration techniques such as evaporation. Firstly, since the separation is generally based on the size differences between milk components and membrane pores, much more control over the final composition of the product is achieved. Secondly, energy consumption of the separation process decreases significantly since there is no need to

* Corresponding Author Email: *mzkazemi@gmail.com*

heat the feed. Last but not least the final quality and nutritional properties of the product is better preserved because the long time heat exposure is eliminated [2, 13].

Unfortunately, the performance of ultrafiltration membrane processes is severely limited by a negative phenomenon called fouling, which is defined as the deposition of solutes on the surface of the membrane or the inner wall of the membrane's pores [14]. This negative phenomenon results in the permeate flux decline over a longer period of time and reduces the efficiency of the filtration process. Major fouling materials in milk solutions are proteins and fats. The size of these molecules is larger than the pores of the membrane, so they are rejected by the membrane and consequently accumulate on the surface of the membrane in the form of a cake layer. Removal of this layer is of vital importance to maintain the performance of the membrane at a desirable level. Therefore, accurate models are needed to predict the fouling at various operational conditions, in order to consider and plan suitable cleaning processes for removing that.

Fouling is heavily dependent on the size of the feed solutes, intrinsic properties of the membrane itself and operational conditions, such as trans-membrane pressure (TMP), temperature and velocity of the feed flow [15, 16]. Thus, working under the optimum operating conditions and also the treatment of the membrane make it possible to remarkably slow the rate of the fouling down. For instance, Ahmad *et al.* used the sol-gel technique to prepare improved antifouling membranes by placing a mesoporous TiO_2 layer on a porous alumina support [16]. They used the treated membrane to analyze the fouling behavior of the model dye compounds in membrane reactors and found that the fouling rate dropped sharply after membrane treatment by this technique.

So far, extensive studies have been conducted to model fouling in membrane contactors using numerical or mathematical methods. These methods either use macroscopic or microscopic models in their simulations [17, 19-22]. Microscopic models focus on solving Navier-Stokes equations along with appropriate boundary and initial conditions. Based on this technique, Reza Kazemi *et al.* proposed a model for concentration distribution of water in ammonia/water solution in a hollow-fiber membrane system. They used COMSOL Multiphysics software to solve Navier-Stokes equations of mass and momentum transfer numerically by Finite Element Method (FEM). Their reported results were in good

agreement with experimental data [22].

In macroscopic models, however, a mathematical equation for flux decline is derived from major fouling mechanisms. These fouling mechanisms include complete blocking mechanism, intermediate blocking mechanism, cake formation mechanism and standard blocking mechanism [17]. According to intermediate or complete pore blocking mechanisms, the available membrane area shrinks with filtered volume, as a consequence of the blockage of the membrane's pores with the feed solutes. These two models are similar to each other, but the assumption behind the complete blocking model is stricter compared with the intermediate blocking model. According to the complete blocking model, the particles seal off the pores without superimposition upon each other. However, the intermediate blocking model alleviates complete blocking mechanism assumption by assuming that some of the solutes block pores and the others superimpose on one another. Standard blocking mechanism assumes that small particles deposit on the inner wall of the membrane's pores, deteriorating the membrane structure and adding additional resistance to the feed flow. This fouling mechanism is considered the most severe fouling, which is very difficult or in many cases impossible to be removed by the usual cleaning processes. According to the cake formation mechanism, particles accumulate on the surface of the membrane in the form of a permeable cake layer, adding an excess resistance to flow [18]. Previous studies on ultrafiltration separation processes showed that this fouling mechanism is the major mechanism responsible for ultrafiltration fouling in wastewater treatment, milk concentration and nitrogen removal [13, 14]. However, there are more than one individual fouling mechanisms involved in the flux decline. Therefore, great attention has been paid to the combination of these mechanisms and their simultaneous effects on flux loss. In this regard, Ho and Zydney [25] developed a mathematical model for flux decline during the purification of bovine serum albumin solution, which accounted for initial fouling by complete blocking and consequently by cake formation mechanism. Their proposed mathematical model, which explicitly described the inhomogeneity in the cake layer due to the complete blocking mechanism was the first model presented for the combined effects of fouling mechanisms and was in good harmony with the empirical data.

Following Ho and Zydney modeling work, a method was utilized to develop combined models

of fouling with two fitted parameters [17]. The method was to insert explicit equations of resistance and available membrane area as a function of time or filtered volume into Darcy's equation. The equations then were integrated to obtain explicit equations of permeate volume as a function of time in constant pressure operation or pressure as a function of time in constant flow operation. The two fouling mechanisms were assumed to occur simultaneously. Based on this method, five models were developed that explained the combined effects of cake filtration-complete blocking, cake filtration-intermediate blocking, complete-standard blocking, intermediate-standard blocking, and cake filtration-standard blocking. The models then were compared with experimental data during microfiltration and ultrafiltration of bovine serum albumin and human IgG. The authors found that these models provided better predictions of flux decline compared to individual fouling mechanisms. Their findings also showed that the combined cake filtration-complete blocking model provided the best data fit for fouling of biological fluids.

Briao and Tavares also used macroscopic modeling in their analysis and found that the data for the fouling of dairy wastewater in tubular ultrafiltration membrane could be fitted initially by the complete blocking and subsequently by the cake formation mechanism [23]. They also found that the cake filtration mechanism was the main mechanism responsible for fouling in spiral wound membranes.

Another fouling modeling was conducted by Corbaton-Baguena *et al.* [24] who fitted an exponential model to the data for the fouling of polyethylene glycol aqueous solution. By taking concentration polarization, particle accumulation on the surface of the membrane and long-term fouling into consideration, they found that this model gave accurate predictions of the fouling in harsh operational conditions.

As understood, cake filtration model and combined cake formation-complete blocking model are the major models in ultrafiltration membrane's fouling. In this study, these two models were used to analyze the flux decline during skim milk concentration at various TMPs and temperatures. These models were compared with each other to provide a deeper insight into the fouling mechanisms involved in this process. Simulations were carried out by CurveExpert Professional software version 1.6 that is a powerful tool for fitting mathematical equations to the experimental data. Permeate volume equations

proposed by Bolton *et al.* were differentiated to obtain flux equations as a function of separation time. Then, the equations were fitted to the empirical data using CurveExpert Professional software. Two different sets of skim milk ultrafiltration data were used here. The first set of data was obtained from testing under constant temperature and flow rate operations with reconstituted skim milk solution. Reconstituted skim milk was filtered through a spiral wound ultrafiltration membrane module. The effect of varying trans-membrane pressures on flux and total hydraulic resistance was then studied. The simulation results revealed that the combined cake filtration-complete blocking model was in excellent agreement with experimental data for skim milk concentration by spiral wound ultrafiltration membrane module, providing a better prediction of flux decline compared to cake filtration model. The second set of experimental data was obtained from partially skimmed milk concentration testing through a Pellicon cassette ultrafiltration membrane module. Unlike the first experiment, the combined cake filtration-complete blocking model was not capable of predicting flux decline and failed catastrophically by CurveExpert software (so there is no curve for this model in the final results) while the cake formation model was in excellent agreement with data sets.

The resistance data was also modeled using Bolton *et al.* proposed resistance equations of standard blocking model and cake filtration model. The results indicated that standard blocking model predictions were incompatible with experimental data and thus was not appropriate for predicting resistance. However, cake filtration model was in good accordance with the resistance empirical data and can be used to solutions whose solutes have a similar behavior to the milk components.

Modeling

The flow rate can be calculated according to the Darcy's law

$$Q = \frac{dV}{dt} = \frac{PA}{R\mu} \qquad (1)$$

where P is the trans-membrane pressure (Pa), μ is the viscosity of feed solution (Pa.s), A is the membrane area (m²) and R is the resistance (m⁻¹).

Complete blocking model

In this model, it is assumed that membrane consists of parallel pores with constant radius and

J. Water Environ. Nanotechnol., 2(4): 311-324 Autumn 2017

313

length and that each solid particle arriving at the membrane blocks a portion of the pores, without superimposition of particles on one another. The following equation shows the relationship between available membrane area and filtered volume [18]

$$\frac{A}{A_0} = 1 - \frac{C_{cb}}{J_0}V \tag{2}$$

Where C_{cb}, A_0 and J_0 denote fitted parameter constant for complete blocking model (s^{-1}), initial membrane frontal area (m^2) and initial flux (m/s), respectively. The equation can be used both in constant flow rate and constant trans-membrane pressure conditions.

At constant flow rate conditions, Eq. (2) can be written as a function of time [17]

$$\frac{A}{A_0} = 1 - C_{cb}t \tag{3}$$

By inserting Eq. (2) into Darcy's law and integrating, the equation of permeate volume as a function of time can be obtained [17]

$$V = \frac{J_0}{C_{cb}}(1 - \exp(-C_{cb}t)) \tag{4}$$

This equation can then be differentiated to obtain the equation for flux in terms of processing time

$$J = J_0 \exp(-C_{cb}t) \tag{5}$$

Cake filtration model

In the cake filtration model, it is assumed that particles accumulate on the surface of the membrane and superimpose upon each other in the form of a permeable cake. As the thickness of the cake increases with time so does the resistance to flow. Therefore, the resistance of the cake layer along with the membrane intrinsic resistance contributes to the total resistance. The total resistance increases with permeate volume according to Eq. (6) and with time according to Eq. (7) [17]

$$\frac{R}{R_0} = 1 + C_{cf}J_0V \tag{6}$$

$$\frac{R}{R_0} = \sqrt{1 + 2C_{cf}J_0^2t} \tag{7}$$

where C_{cf} denotes cake filtration constant parameter which has units of s.m^{-2}. The filtered volume can be obtained from the following equation [17]

$$V = \frac{1}{C_{cf}J_0}(\sqrt{1 + 2C_{cf}J_0^2t} - 1) \tag{8}$$

This equation can then be differentiated to obtain equation for flux as a function of time

$$J = J_0(1 + 2C_{cf}J_0^2t)^{-0.5} \tag{9}$$

Standard blocking model

In this model, it is assumed that membrane consists of straight cylindrical pores whose radius decreases with time due to the accumulation of solid particles on the pore walls of the membrane [18, 26]. The following equations show the relationship between resistance and volume (Eq. (10)) or time (Eq. (11)) [17]

$$\frac{R}{R_0} = (1 - \frac{C_{sb}V}{2})^{-2} \tag{10}$$

$$\frac{R}{R_0} = (1 + \frac{C_{sb}J_0t}{2})^2 \tag{11}$$

In these equations, constant C_{sb} denotes fitted parameter for standard blocking model with units of m^{-1}. The equation of permeate volume as a function of time thus can be obtained [17]

$$V = (\frac{1}{J_0t} + \frac{C_{sb}}{2})^{-1} \tag{12}$$

Combined cake filtration-complete blocking model

Bolton *et al.* developed a combined model based on the effects of pore blockage and cake formation mechanisms. Filtration area loss predicted by the complete blocking mechanism was combined with the resistance from caking. By inserting Eq. (2) and Eq. (7) into Darcy's equation, the equation for volume filtered as a function of time can be obtained [17]

$$V = \frac{J_0}{C_{cb}}(1 - \exp\left(\frac{-C_{cb}}{C_{cf}J_0^2}((1 + 2C_{cf}J_0^2t)^{0.5} - 1)\right)) \tag{13}$$

The equation can then be differentiated to determine the equation for flux in terms of time

$$J = J_0 \exp\left(\frac{-C_{cb}}{C_{cf}J_0^2}\left((1 + 2C_{cf}J_0^2t)^{0.5} - 1\right)\right)$$
$$/(1 + 2C_{cf}J_0^2t)^{0.5} \tag{14}$$

In case of caking, the equations of resistance (R) versus time, Eq. (7), was used. The equation of R as a function of V cannot be used here since volume filtered is defined relative to the available membrane area which is declining during the experiment.

In case of complete blocking, the equation of area in terms of volume filtered was used. The equation of area loss as a function of time is not

314

J. Water Environ. Nanotechnol., 2(4): 311-324 Autumn 2017

valid here since the rate of complete blocking with respect to time is slower than cake formation. A detailed description of these models is provided by Bolton *et al.* [17].

A summary of these models is provided in Table 1.

EXPERIMENTAL

Skim milk ultrafiltration using a spiral wound module

The experimental data sets used in this paper were obtained from previous studies of skim milk ultrafiltration done by Razavi *et al.* [19]. They used a spiral wound membrane ultrafiltration unit (Biocon company, Moscow, Russia). The membrane material was polysulfone amide with a 20-kDa molecular weight cut off.

The membrane system was equipped with a tubular heat exchanger and a temperature sensor was applied to keep the feed at a constant temperature of 40 °C. Membrane unit was also installed to a feed tank (20 L) and a flow meter measured the feed flow rate which was held constant at 15 L.min^{-1} [19].

The membrane's length, inner radius, and surface area were 0.47 m, 0.11 m and 0.33 m^2, respectively.

Two pressure gauges measured inlet pressure (P_{in}) and outlet pressure (P_{out}). The TMP was obtained by the following equation [19]

$$TMP = \frac{1}{2}(P_{in} + P_{out}) - P_{permeate} \qquad (15)$$

The feed solution was prepared by mixing skim milk powder with water at a temperature of about 50 °C in a blender. The final pH of the feed was obtained to be 6.54. The average content of the total solid (TS) and water in produced solution was 8.443 and 91.557 %, respectively. Experiments were carried out at different TMPs (50, 100, 150, 200 and 250 kPa) to investigate the effect of pressure on flux decline. All experimental runs repeated twice. For each filtration run, the water was first contacted with the membrane to measure water flux. Membrane intrinsic resistance then was calculated according to Darcy's law [19]

$$R_{i,m} = \frac{TMP}{\mu_{permeate} \ J_{permeate}} \qquad (16)$$

where $\mu_{permeate}$ denotes permeate dynamic viscosity (water dynamic viscosity) (Pa.s) and $R_{i,m}$ denotes membrane intrinsic resistance (m^{-1}). In the next step, the water was replaced with reconstituted skim milk at 40 °C. The permeate flux was measured and recorded every 30 s.

After 30 min filtration, the operation was stopped and the membrane system was cleaned by distilled water and NaOH solution according to the protocol described by the manufacturer.

Skim milk ultrafiltration using a Pellicon cassette module

Rinaldoni *et al.* used a Pellicon cassette membrane ultrafiltration unit (Millipore, USA) [27]. The membrane material was modified polysulfone with 10-kDa molecular weight cut off and total membrane surface area of 0.5 m^2.

The feed solution (partially skimmed milk supplied by MILKAUT) was first heated in a water bath. It was then pumped through the membrane system with a constant feed flow rate of 29 ± 0.05 L.min^{-1}.

The effect of different pressures (0.5, 1 and 1.5 bar) and different temperatures (20, 30 and 40 °C) on flux was investigated. All experiments were carried out twice.

RESULTS

Skim milk concentration with spiral wound ultrafiltration module

The combined cake filtration-complete blocking model was compared with individual cake filtration model and experimental data for the concentration of skim milk. Experiments were performed using a polysulfone amide ultrafiltration membrane with twelve kilograms of reconstituted skim milk at constant temperature and flow rate (40 °C and 15 L.min^{-1}, respectively) [19]. To investigate the effect of pressure on flux decline, experiments were carried out at 50, 100, 150, 200 and 250 kPa transmembrane pressures. The permeate flux and total

Table 1: Summary of the equations of cake filtration model, complete blocking model and combined cake-complete blocking model.

Model	Equation	Fitted parameters
Complete blocking (Eq. (5))	$J = J_0 \exp(-C_{cb}t)$	C_{cb} (s^{-1})
Cake filtration (Eq. (9))	$J = J_0(1 + 2C_{cf}J_0^2 t)^{-0.5}$	C_{cf} (s.m^{-2})
Cake-complete (Eq. (14))	$J = J_0 \exp\left(\frac{-C_{cb}}{C_{cf}J_0^2}\left((1 + 2C_{cf}J_0^2 t)^{0.5} - 1\right)\right)/(1 + 2C_{cf}J_0^2 t)^{0.5}$	C_{cf} (s.m^{-2}), C_{cb} (s^{-1})

J. Water Environ. Nanotechnol., 2(4): 311-324 Autumn 2017

315

resistance were measured as a function of time and recorded every 30 s.

The flux data and the model predictions for skim milk samples at different pressures are shown in Fig. 1. The combined cake filtration-complete blocking model (solid green lines) provided the best fits of the flux data at moderate pressures (100 and 150 kPa) with error values remarkably lower than
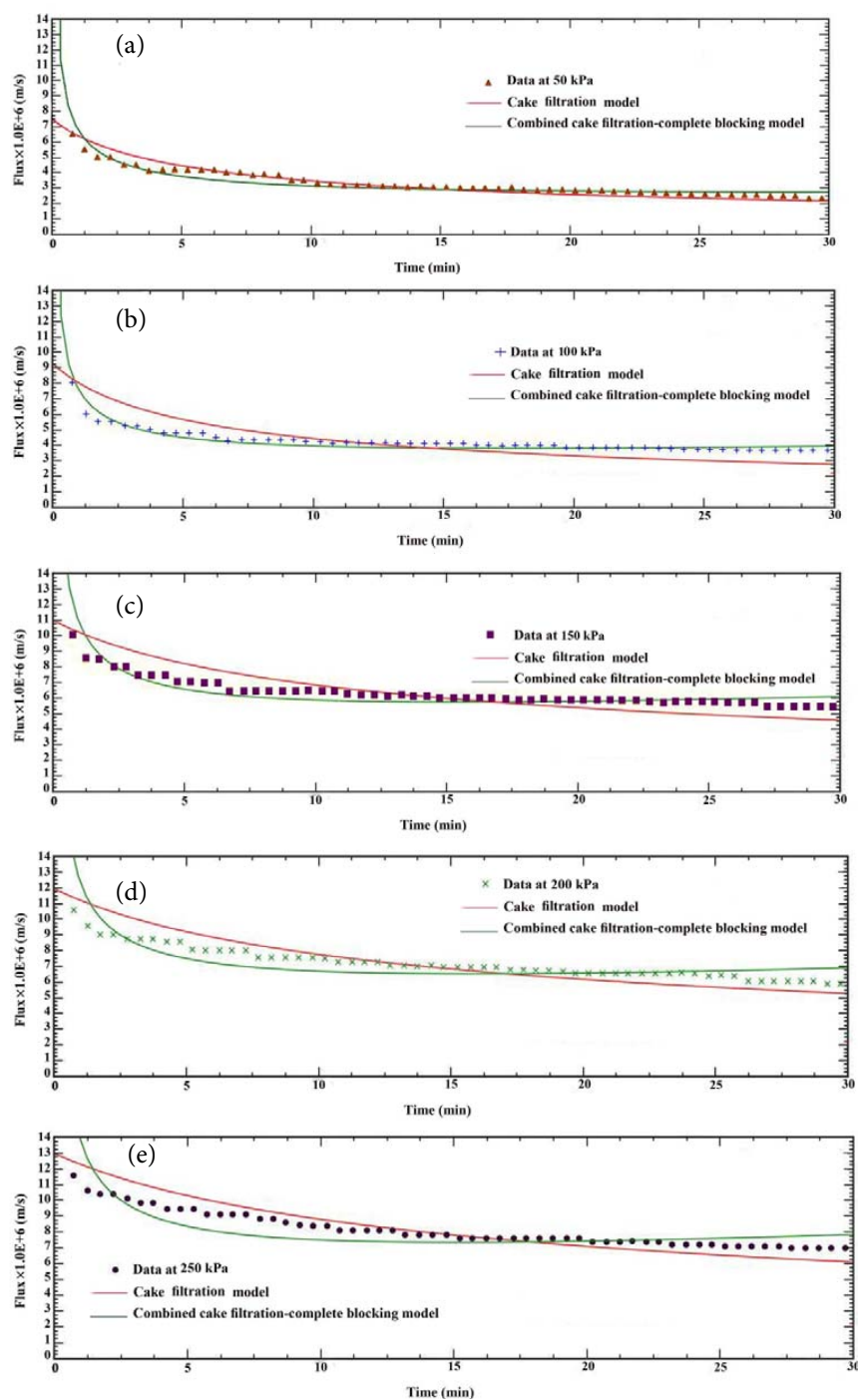

Fig. 1: Flux vs. time data for skim milk through spiral wound ultrafiltration membrane module compared to the cake formation model and combined cake filtration-complete blocking model: (a) 50 kPa, (b) 100 kPa, (c) 150 kPa, (d) 200 kPa and (e) 250 kPa.

316

J. Water Environ. Nanotechnol., 2(4): 311-324 Autumn 2017

the individual cake filtration model (Fig. 1(b) and (c), Table 2). At high and low pressures, however, the error values of the combined cake filtration-complete blocking model were slightly higher than the individual cake formation model. This behavior can be attributed to the prevalent effect of cake formation mechanism at higher TMPs and negligible complete blocking mechanism effects. This could be accurate, since high TMPs will result in a more compact cake layer, with pore inlets much smaller to be blocked by particles, which tend to seal off membrane pores in a complete blocking manner.

Values of C_{cb} and C_{cf} were applied to evaluate the contributions of complete blocking and cake formation to the combined cake formation-complete blocking model. The small value of $\frac{-C_{cb}}{C_{cf}J_0^2}$ which was approximately 0, indicated that the contributions of the two individual mechanisms were similar.

Since milk solution has distinct species with various size and shape, probably the fouling is caused by caking of large molecules such as proteins and fats arriving at the membrane earlier in the run. Fouling then will be followed by complete blocking of smaller particles like microorganisms. These particles can go through the cake, reach

the membrane surface and seal off membrane pores. Thus complete blockage occurs at the end of the experiment. As it can be seen from Table 2, with increasing trans-membrane pressure the differences between experimental data and models generally increased. This behavior can be attributed to other mechanisms involved in fouling at higher pressures, like diffusion of small particles through the cake layer. Thus a fifth mechanism must be considered at higher pressures, which is expected to be investigated at further works.

The results of total resistance data modeling are shown in Fig. 2. Since the resistance data at 150 kPa and 100 kPa were very close to each other, only data at 100 kPa are shown and modeled. As it can be seen from the figure, standard blocking model was poor in predicting resistance to flow (dashed green lines), while cake formation resistance (solid red lines) was in agreeable agreement with the resistance data for skim milk at lower pressures with low error values, as seen in Table 3.

In ultrafiltration of skim milk, the fouling is begun with an accumulation of large particles like proteins and fats in the form of a cake layer on the surface of the membrane. Smaller particles then will settle down on top of this layer. Therefore, the cake filtration mechanism seems to be the main mechanism in

Table 2: Combined cake filtration-complete blocking and cake filtration model standard error values and fitted parameters of skim milk concentration using spiral wound ultrafiltration membrane module at different TMPs.

Model	Model standard error	Fit parameter values
Cake-complete (Eq. (14))	3.19×10^{-1}	$C_{cb} = -6.26 \times 10^{11}$ s^{-1} (50 kPa), $C_{cf} = 8.16 \times 10^{16}$ s.m^{-2} (50 kPa)
	2.61×10^{-1}	$C_{cb} = -4.09 \times 10^{11}$ s^{-1} (100 kPa), $C_{cf} = 3.10 \times 10^{16}$ s.m^{-2} (100 kPa)
	4.95×10^{-1}	$C_{cb} = -1.90 \times 10^{11}$ s^{-1} (150 kPa), $C_{cf} = 8.16 \times 10^{15}$ s.m^{-2} (150 kPa)
	7.60×10^{-1}	$C_{cb} = -1.26 \times 10^{11}$ s^{-1} (200 kPa), $C_{cf} = 4.40 \times 10^{15}$ s.m^{-2} (200 kPa)
	8.73×10^{-1}	$C_{cb} = -9.24 \times 10^{10}$ s^{-1} (250 kPa), $C_{cf} = 2.61 \times 10^{15}$ s.m^{-2} (250 kPa)
Cake filtration (Eq. (9))	2.97×10^{-1}	$C_{cf} = 5.32 \times 10^{7}$ s.m^{-2} (50 kPa)
	7.41×10^{-1}	$C_{cf} = 3.19 \times 10^{7}$ s.m^{-2} (100 kPa)
	7.66×10^{-1}	$C_{cf} = 1.08 \times 10^{7}$ s.m^{-2} (150 kPa)
	6.86×10^{-1}	$C_{cf} = 7.86 \times 10^{6}$ s.m^{-2} (200 kPa)
	6.73×10^{-1}	$C_{cf} = 5.72 \times 10^{6}$ s.m^{-2} (250 kPa)

Table 3: Standard blocking and cake filtration model standard error values and fitted parameters of total resistance in skim milk concentration using spiral wound ultrafiltration membrane module at different TMPs.

Model	Model standard error	Fit parameter values
Standard blocking (Eq. (11))	4.90×10^{-1}	$C_{sb} = 1.93 \times 10^{2}$ m^{-1} (50 kPa)
	9.33×10^{-1}	$C_{sb} = 1.36 \times 10^{2}$ m^{-1} (100 kPa)
	8.00×10^{-1}	$C_{sb} = 7.83 \times 10^{1}$ m^{-1} (200 kPa)
	8.88×10^{-1}	$C_{sb} = 6.85 \times 10^{1}$ m^{-1} (250 kPa)
Cake filtration (Eq. (7))	1.99×10^{-1}	$C_{cf} = 9.73 \times 10^{7}$ s.m^{-2} (50 kPa)
	5.49×10^{-1}	$C_{cf} = 5.09 \times 10^{7}$ s.m^{-2} (100 kPa)
	4.89×10^{-1}	$C_{cf} = 1.66 \times 10^{7}$ s.m^{-2} (200 kPa)
	5.50×10^{-1}	$C_{cf} = 1.29 \times 10^{7}$ s.m^{-2} (250 kPa)

J. Water Environ. Nanotechnol., 2(4): 311-324 Autumn 2017
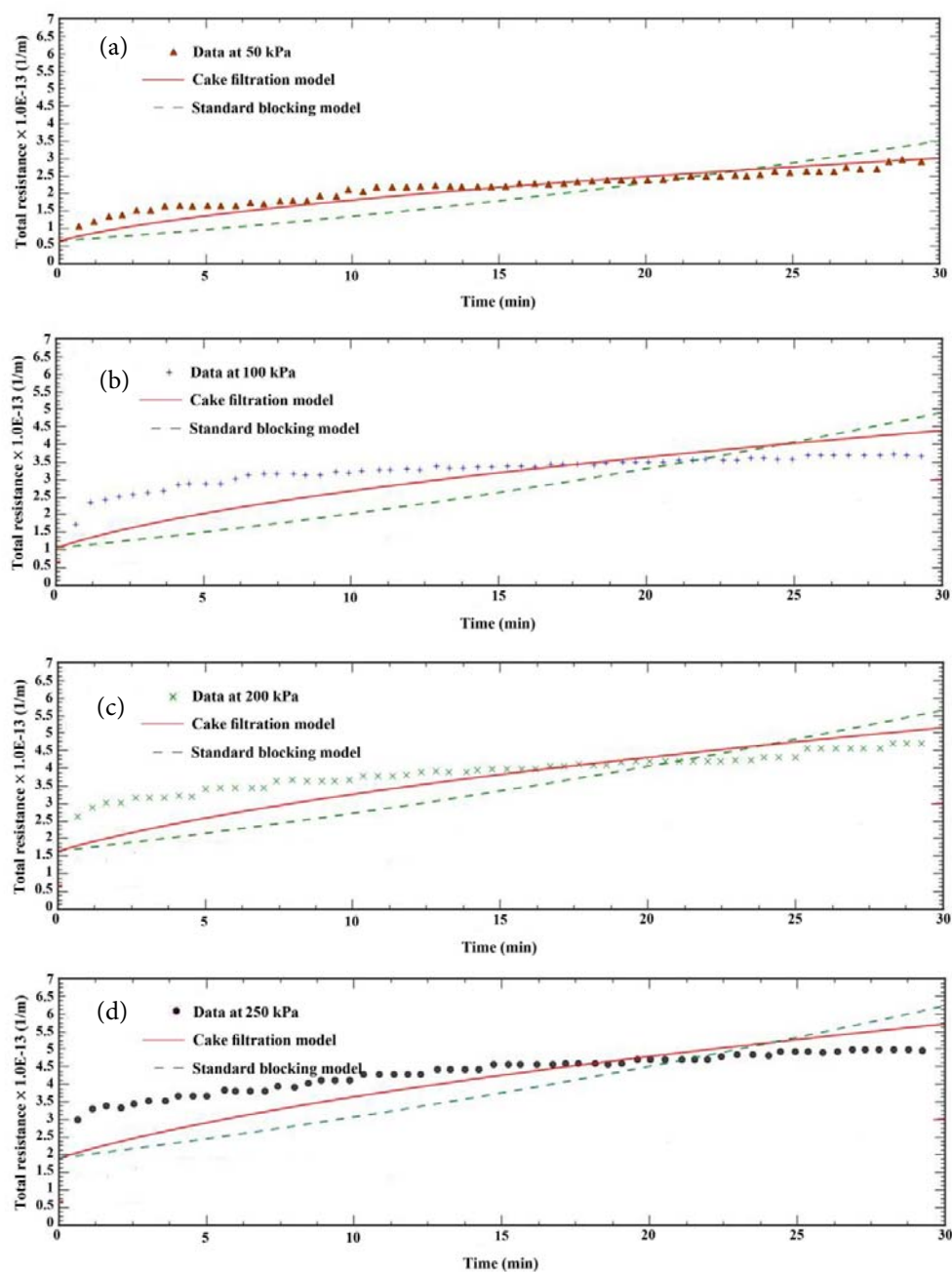
317

Fig. 2: Resistance vs. time data compared to the cake formation model and standard blocking model: (a) 50 kPa, (b) 100 kPa, (c) 200 kPa and (d) 250 kPa.

this process which appropriately predicts fouling behavior. This was verified by the poor predictions of the standard blocking model and good predictions of total resistance due to the cake formation mechanism.

The calculated fitted parameters versus iteration using CurveExpert are shown in Fig. 3. As it can be seen in the figure, the number of iterations used for calculating fitted parameters was more than 40 and 15 for combined cake filtration-complete blocking model (Fig. 3(a)) and cake filtration model (Fig. 3(b) and (c)), respectively. This means that CurveExpert is converged after more than 40 and 15 iterations for these models. According to Fig. 3(d), after approximately 2 to 3 iterations, a fitted parameter for the standard blocking model is not changed. This means that CurveExpert is converged after

318

J. Water Environ. Nanotechnol., 2(4): 311-324 Autumn 2017
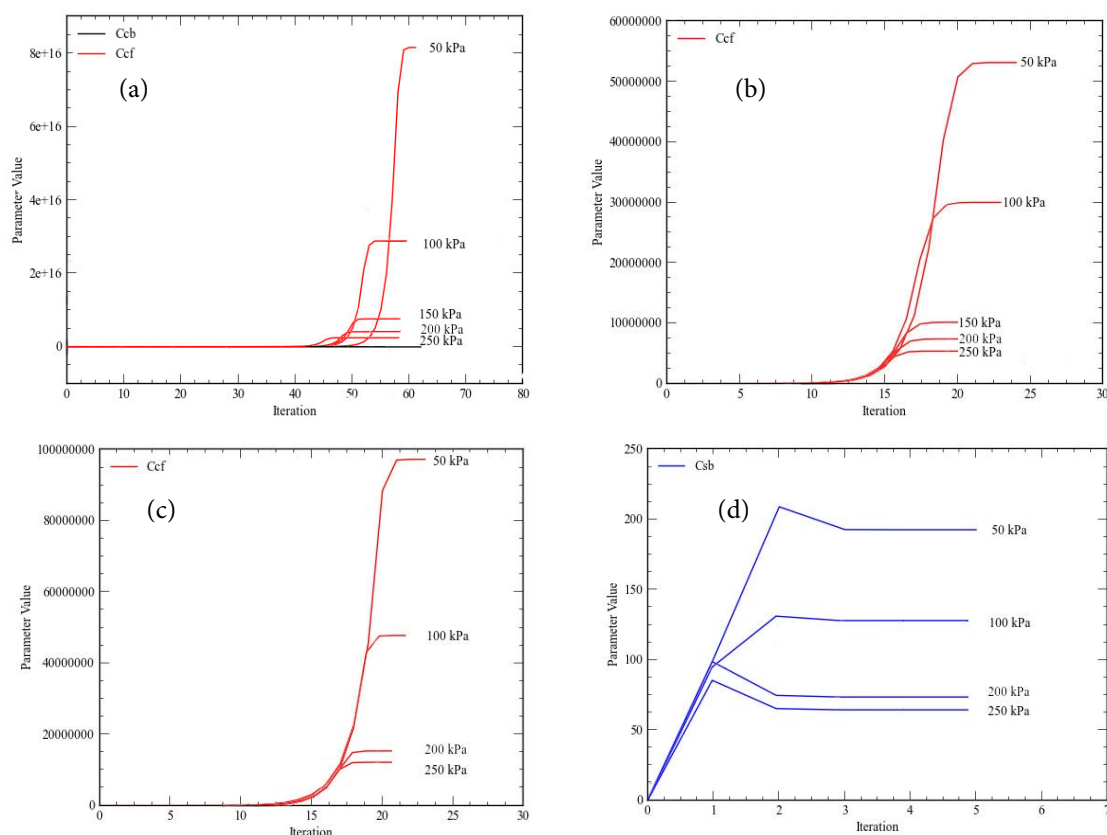
Fig. 3: Calculated fitted parameters vs. iteration by CurveExpert: (a) cake filtration-complete blocking flux prediction, (b) cake formation flux prediction, (c) cake formation resistance prediction and (d) standard blocking resistance prediction.
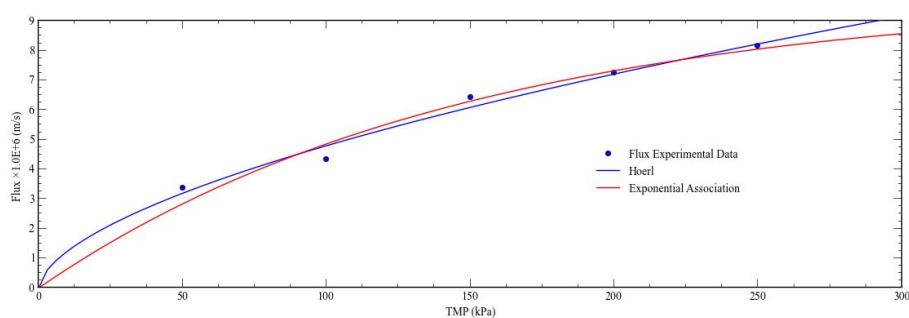

Fig. 4: Averaged data values of flux vs. TMP for skim milk through spiral wound ultrafiltration membrane module compared to Hoerl and Exponential Association regressions.

approximately 2 to 3 iterations for standard blockage mechanism.

Fig. 4 and 5 show the effect of different trans-membrane pressures on flux and total resistance, respectively. Averaged values of flux and resistance were used and the data was modeled using Hoerl and Exponential Association regressions. For Hoerl regression (blue solid line), the following equation

was used

$$Y = ab^x x^c \qquad (17)$$

In which Y denotes either flux or resistance, x denotes TMP and a, b and c are constant parameters. These parameters are obtained by regression and their values are shown in Table 4 and 5 for flux and resistance data, respectively. For Exponential Association regression, the following

J. Water Environ. Nanotechnol., 2(4): 311-324 Autumn 2017

319

equation was used

$$Y = a(1 - e^{-bx}) \tag{18}$$

As it can be seen from Fig. 4, flux increased by TMP. Both regressions were in excellent agreement with actual values. However, predictions of Hoerl regression were better for flux prediction with error values slightly lower than Exponential Association regression (Table 4). For resistance prediction (Fig. 5), two regressions were approximately the same.

Skim milk concentration with Pellicon cassette ultrafiltration module

Experiments were performed using a modified polysulfone ultrafiltration membrane with partially skimmed milk at constant flow rate (29 ± 0.05 L.min^{-1}) [27]. To investigate the effect of pressure

on flux decline, experiments were carried out at 0.5, 1 and 1.5 bar trans-membrane pressures. The effect of different temperatures (20, 30 and 40 °C) on flux decline was also investigated.

The combined cake filtration-complete blocking model failed catastrophically by CurveExpert Professional, so there is no curve for this model in the final results. The flux data at different pressures and different temperatures thus was modeled using only cake filtration model. Applying cake formation mechanism resulted in a very good data fit. The flux data and the model predictions for skim milk samples at different pressures and different temperatures are shown in Fig. 6 and 7, respectively.

As it can be seen from Table 6, standard errors for the cake filtration model were almost the same at
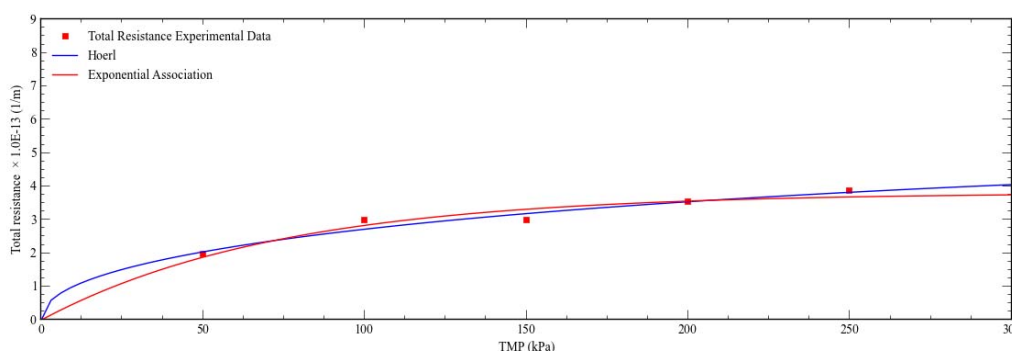

Fig. 5: Averaged data values of total resistance vs. TMP for skim milk through spiral wound ultrafiltration membrane module compared to Hoerl and Exponential Association regressions.

Table 4: Hoerl and Exponential Association regression standard error values and constant parameters for the flux data of skim milk concentration using spiral wound ultrafiltration membrane module at different TMPs.

Regression	Regression standard error	a	b	c
Hoerl	4.43×10^{-1}	3.22×10^{-1}	1	5.85×10^{-1}
Exponential Association	4.54×10^{-1}	9.86	6.77×10^{-3}	

Table 5: Hoerl and Exponential Association regression standard error values and constant parameters for the total resistance data of skim milk concentration using spiral wound ultrafiltration membrane module at different TMPs.

Regression	Regression standard error	a	b	c
Hoerl	2.44×10^{-1}	3.62×10^{-1}	9.99×10^{-1}	4.47×10^{-1}
Exponential Association	2.42×10^{-1}	3.81	1.36×10^{-2}	

Table 6: Cake formation model standard error values and fitted parameter of flux data in partially skimmed milk concentration using Pellicon cassette ultrafiltration membrane module at different TMPs and temperatures.

Model	Model standard error	Fit parameter values
Cake filtration (Eq. (9))	1.30×10^{-1}	$C_{cf} = 1.88 \times 10^{8}$ s.m^{-2} (0.5 bar)
	1.55×10^{-1}	$C_{cf} = 7.63 \times 10^{7}$ s.m^{-2} (1 bar)
	1.33×10^{-1}	$C_{cf} = 3.11 \times 10^{7}$ s.m^{-2} (1.5 bar)
	2.10×10^{-1}	$C_{cf} = 1.09 \times 10^{8}$ s.m^{-2} (20 °C)
	2.02×10^{-1}	$C_{cf} = 9.42 \times 10^{7}$ s.m^{-2} (30 °C)
	1.98×10^{-1}	$C_{cf} = 7.15 \times 10^{7}$ s.m^{-2} (40 °C)

different trans-membrane pressures. This indicates that TMP had no significant effect on simulation of flux decline for ultrafiltration of partially skimmed milk.

The calculated cake filtration fitted parameter versus iteration using CurveExpert is shown in Fig. 8. As it can be seen in this figure, the number of iterations used for calculating fitted parameters in cake filtration model was more than 15. This means that, after more than 15 iterations, cake filtration fitted parameter has not changed and CurveExpert is converged.

The effect of different trans-membrane pressures

and temperatures on flux decline is shown in Fig. 9 and 10, respectively. Averaged values of flux were used and the data of flux versus TMP and temperature was modeled using Modified Power and Geometric regressions. For Modified Power regression, the following equation was used

$$Y = ab^x \tag{19}$$

For Geometric regression, the following equation was used
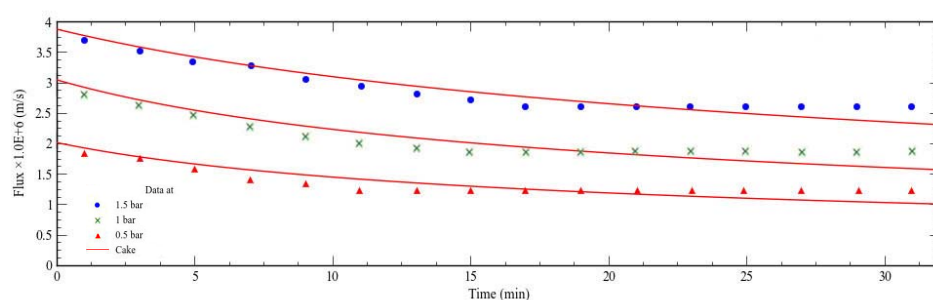
$$Y = ax^{bx} \tag{20}$$

Fig. 6: Flux vs. time data for skim milk through Pellicon cassette ultrafiltration membrane module compared to the cake formation model at different TMPs.
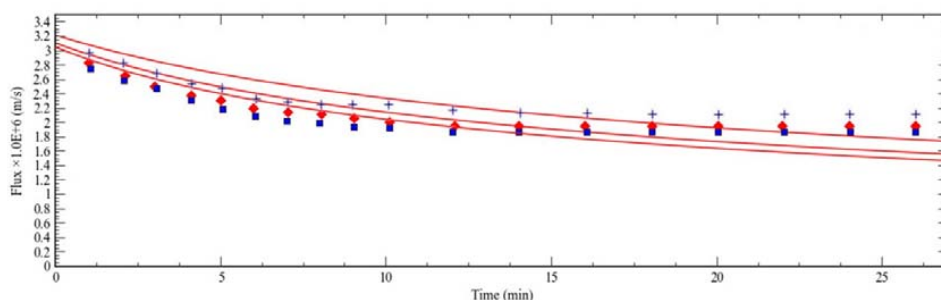

Fig. 7: Flux vs. time data for skim milk through Pellicon cassette ultrafiltration membrane module compared to the cake formation model at different temperatures.
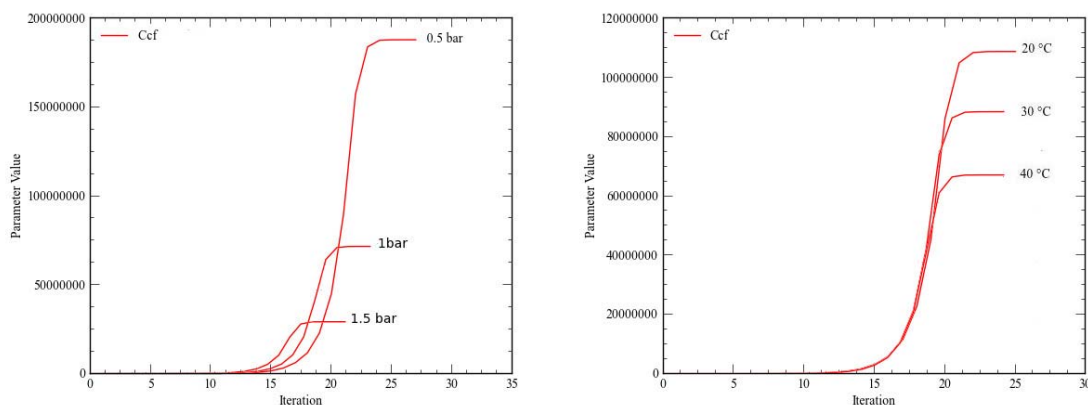

Fig. 8: Calculated cake formation fitted parameter vs. iteration by CurveExpert at different pressures (a) and different temperatures (b).

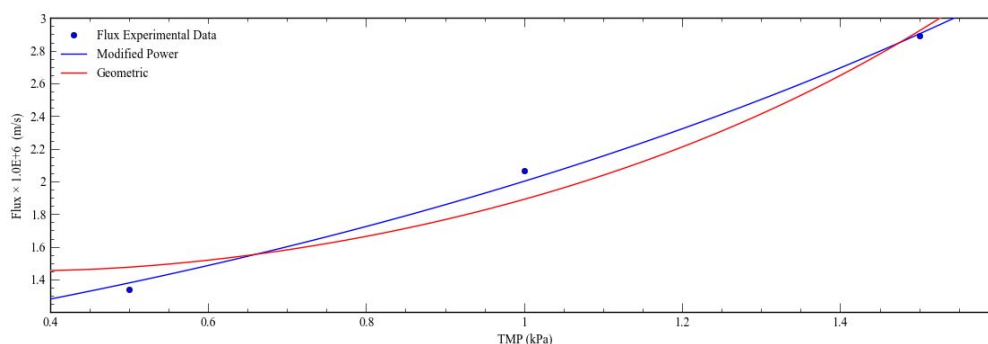*J. Water Environ. Nanotechnol., 2(4): 311-324 Autumn 2017*

321

Fig. 9: Averaged data values of flux vs. TMP for partially skimmed milk through Pellicon cassette ultrafiltration membrane module compared to the Modified Power and Geometric regressions.
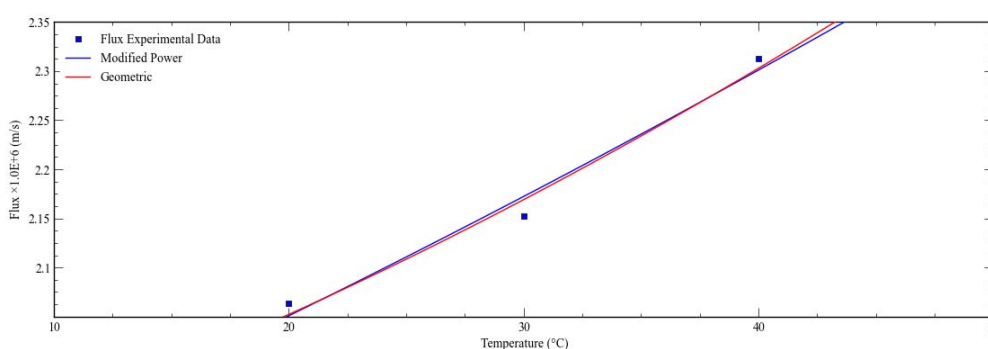

Fig. 10: Averaged data values of flux vs. temperature for partially skimmed milk through Pellicon cassette ultrafiltration membrane module compared to the Modified Power and Geometric regressions.

Table 7: Modified Power and Geometric regression standard error values and constant parameters for the flux data in partially skimmed milk concentration using Pellicon cassette ultrafiltration membrane module at different TMPs.

Regression	Regression standard error	a	b
Modified Power	0.77×10^{-1}	9.56×10^{-1}	2.1
Geometric	2.24×10^{-1}	1.9	7.14×10^{-1}

Table 8: Modified Power and Geometric regression standard error values and constant parameters for the flux data in partially skimmed milk concentration using Pellicon cassette ultrafiltration membrane module at different temperatures.

Regression	Regression standard error	a	b
Modified Power	0.26×10^{-1}	1.83	1
Geometric	0.22×10^{-1}	1.9	1.31×10^{-3}

in which x denotes either TMP or temperature. As it can be seen from the figures, flux grew by TMP and temperature. However, flux growth was higher with a 0.5 bar increase in TMP than a 10 °C increase in temperature. Geometric regression was better for predicting flux versus temperature, with error values slightly lower than Modified Power regression, as shown in Table 8. However, predictions of Modified Power regression were better for predicting flux vs. TMP, with error values considerably lower than Geometric regression error values (Table 7).

CONCLUSIONS

To model fouling in milk concentration process, the combined cake filtration-complete blocking model proposed by Bolton *et al.* and typical cake filtration model were applied to ultrafiltration of skim milk at different TMPs. The combined model used two fitted parameters and simplified to the equations for the typical mechanisms when the effects of second fouling mechanism were negligible.

The applicability of the model to the data for the skim milk concentration at different trans-

membrane pressures was tested. The combined cake filtration-complete blocking model was in excellent accordance with experimental flux data. It was able to predict fouling of skim milk concentration through spiral wound ultrafiltration module and provided good fits compared to individual cake formation mechanism. Thus, the combined cake filtration-complete blocking model can be regarded as an effective model for predicting flux decline in solutions where the volume filtered decreases in a manner between the extremes of cake formation and complete blocking. The results also showed that cake formation model was in good harmony with experimental data for flux decline in ultrafiltration of partially skimmed milk while combined cake formation-complete blocking model failed catastrophically. The results of resistance modeling also showed that the cake formation model provided good fits of the data sets while the standard blocking predictions were poor.

CONFLICT OF INTEREST

The authors declare that there are no conflicts of interest regarding the publication of this manuscript.

Nomenclature

A   available membrane area (m^2)

A_0 initial membrane area (m^2)

a   regression constant parameter

b   regression constant parameter

c   regression constant parameter

C_{cb} complete blocking constant (s^{-1})

C_{cf} cake filtration constant   ($s.m^{-2}$)

J   flux ($m.s^{-1}$)

J_0 initial flux ($m.s^{-1}$)

$J_{permeate}$ permeate flux ($m.s^{-1}$)

P_{in} inlet pressure (Pa)

P_{out} outlet pressure (Pa)

$P_{permeate}$ permeate pressure (Pa)

Q   flow rate ($m^3.s^{-1}$)

R   resistance to flow (m^{-1})

R_0 initial resistance to flow (m^{-1})

$R_{i,m}$ intrinsic membrane resistance (m^{-1})

t   time (s)

TMP   trans-membrane pressure (Pa)

V   permeate volume ($m^3.m^{-2}$)

μ   feed viscosity ($kg.m^{-1}.s^{-1}$)

$μ_{permeate}$ permeate dynamic viscosity ($kg.m^{-1}.s^{-1}$)

REFERENCES

1 GEA Process Engineering, Membrane Filtration in the Dairy Industry, 2015. (http://www.gea.com/global/en/binaries/Membrane) (Accessed 23.06.15).

2. Ng KSY, Haribabu M, Harvie DJE, Dunstan DE, Martin GJO. Mechanisms of flux decline in skim milk ultrafiltration: A review. Journal of Membrane Science. 2017;523(Supplement C):144-62.

3. Sluková M, Hinková A, Henke S, Smrž F, Lukačíková M, Pour V, et al. Cheese whey treated by membrane separation as a valuable ingredient for barley sourdough preparation. Journal of Food Engineering. 2016;172(Supplement C):38-47.

4. Das B, Sarkar S, Sarkar A, Bhattacharjee S, Bhattacharjee C. Recovery of whey proteins and lactose from dairy waste: A step towards green waste management. Process Safety and Environmental Protection. 2016;101(Supplement C):27-33.

5. H. Patel, S. Patel, S. Agarwal, I. Technology, Milk Protein Concentrates: Manufacturing and Application, 2014. (http://www.usdairy.com/~/media/USD/Public/MPC-Tech-Report-FINAL-pdf) (Accessed 20.06.16).

6. Tovar Jiménez X, Arana Cuenca A, Téllez Jurado A, Abreu Corona A, Muro Urista CR. Traditional Methods for Whey Protein Isolation and Concentration: Effects on Nutritional Properties and Biological Activity. Journal of the Mexican Chemical Society. 2012;56:369-77.

7. Cheang B, Zydney AL. Separation of α-lactalbumin and β-lactoglobulin using membrane ultrafiltration. Biotechnology and Bioengineering. 2003;83(2):201-9.

8. Rahimi Z, Zinatizadeh AA, Zinadini S. Milk processing wastewater treatment in a bioreactor followed by an anti-fouling O-carboxymethyl chitosan modified Fe3O4/PVDF ultrafiltration membrane. Journal of Industrial and Engineering Chemistry. 2016;38(Supplement C):103-12.

9. Zin G, Penha FM, Rezzadori K, Silva FL, Guizoni K, Petrus JCC, et al. Fouling control in ultrafiltration of bovine serum albumin and milk by the use of permanent magnetic field. Journal of Food Engineering. 2016;168(Supplement C):154-9.

10. Crowley SV, O'Callaghan TF, Kelly AL, Fenelon MA, O'Mahony JA. Use of ultrafiltration to prepare a novel permeate for application in the functionality testing of infant formula ingredients. Separation and Purification Technology. 2015;141(Supplement C):294-300.

11. Lin MJ, Grandison AS, Lewis MJ. Partitioning of calcium and magnesium (total divalent cations) during membrane filtration of milk. Journal of Food Engineering. 2015;149(Supplement C):153-8.

12. Zhang W, Ding L. Investigation of membrane fouling mechanisms using blocking models in the case of shear-enhanced ultrafiltration. Separation and Purification Technology. 2015;141(Supplement C):160-9.

13. Aslam M, Lee P-H, Kim J. Analysis of membrane fouling with porous membrane filters by microbial suspensions for autotrophic nitrogen transformations. Separation and Purification Technology. 2015;146(Supplement C):284-93.

14. Charfi A, Ben Amar N, Harmand J. Analysis of fouling mechanisms in anaerobic membrane bioreactors. Water Research. 2012;46(8):2637-50.

15. Rezaei H, Ashtiani FZ, Fouladitajar A. Fouling behavior and performance of microfiltration membranes for whey treatment in steady and unsteady-state conditions. Brazilian Journal of Chemical Engineering. 2014;31:503-18.

16. Ahmad R, Kim JK, Kim JH, Kim J. Well-organized, mesoporous nanocrystalline TiO2 on alumina membranes with

J. Water Environ. Nanotechnol., 2(4): 311-324 Autumn 2017

323

hierarchical architecture: Antifouling and photocatalytic activities. Catalysis Today. 2017;282(Part 1):2-12.

17. Bolton G, LaCasse D, Kuriyel R. Combined models of membrane fouling: Development and application to microfiltration and ultrafiltration of biological fluids. Journal of Membrane Science. 2006;277(1):75-84.

18. Hermia J. Constant Pressure Blocking Filtration Law Application to Powder-Law Non-Newtonian Fluid. Trans Inst Chem Eng. 1982;60:183-7.

19. Razavi MA, Mortazavi A, Mousavi M. Dynamic modelling of milk ultrafiltration by artificial neural network. Journal of Membrane Science. 2003;220(1):47-58.

20. Mignard D, Glass DH. Fouling during the cross-flow ultrafiltration of proteins: a mass-transfer model. Journal of Membrane Science. 2001;186(1):133-43.

21. Marcos B, Moresoli C, Skorepova J, Vaughan B. CFD modeling of a transient hollow fiber ultrafiltration system for protein concentration. Journal of Membrane Science. 2009;337(1):136-44.

22. Rezakazemi M, Shirazian S, Ashrafizadeh SN. Simulation of ammonia removal from industrial wastewater streams by means of a hollow-fiber membrane contactor. Desalination. 2012;285(Supplement C):383-92.

23. Brião VB, Tavares CRG. Pore blocking mechanism for the recovery of milk solids from dairy wastewater by ultrafiltration. Brazilian Journal of Chemical Engineering. 2012;29:393-407.

24. Corbatón-Báguena M-J, Vincent-Vela M-C, Álvarez-Blanco S, Lora-García J. Analysis of Two Ultrafiltration Fouling Models and Estimation of Model Parameters as a Function of Operational Conditions. Transport in Porous Media. 2013;99(2):391-411.

25. Ho C-C, Zydney AL. Transmembrane pressure profiles during constant flux microfiltration of bovine serum albumin. Journal of Membrane Science. 2002;209(2):363-77.

26. Grace HP. Structure and performance of filter media. II. Performance of filter media in liquid service. AIChE Journal. 1956;2(3):316-36.

27. Rinaldoni AN, Tarazaga CC, Campderrós ME, Padilla AP. Assessing performance of skim milk ultrafiltration by using technical parameters. Journal of Food Engineering. 2009;92(2):226-32.

324

J. Water Environ. Nanotechnol., 2(4): 311-324 Autumn 2017